Investigating the antibacterial activity and mode of action of antimicrobial peptides Os and Os-C against Staphylococcus epidermidis

Jonathan Odingo[1], Megan J Bester[1], Anabella R.M Gaspar[1], and Helena Taute[1]

[1]Affiliation not available

September 8, 2022

Abstract

This study sought to investigate the antibacterial activity and mode of action of two antimicrobial peptides, Os and Os-C, derived from a soft tick defensin against *Staphylococcus epidermidis*. The antibacterial activity of both peptides was investigated in 1% tryptic soy broth medium and Os and Os-C had a minimum inhibitory concentration of 3.43 µM and 10 µM, respectively. Both peptides were able to cause 99.5% killing at 10 µM following three hours of treatment. The mode of action of the two peptides was also investigated using the Live/Dead membrane permeability kit in addition to a membrane potential sensitive dye, $DiBAC_4(3)$. It was shown that both melittin and Os caused membrane permeabilisation at 0.4 µM and 7 µM, respectively, whereas Os-C did not cause permeabilisation at 20 µM. Os and Os-C were further shown to affect membrane potential by causing membrane depolarisation. Further visualisation of the cells using scanning and transmission electron microscopy revealed that both Os and Os-C including melittin adversely affected the *S. epidermidis* membrane causing membrane blebbing, indentation with Os and melittin inducing ghost cell formation. Transmission electron microscopy further revealed that Os was lytic whereas Os-C induced mesosome formation, a possible consequence of reactive oxygen species production. Both peptides were thus active against the pathogen with further development necessary for increased activity and stability of Os and Os-C against *S. epidermidis*.

Introduction

Antimicrobial resistance (AMR) continues to strain healthcare systems with low-and-middle income countries bearing the brunt of the issue. The Lancet published an AMR surveillance report in 2019 where 4.95 million deaths were associated with AMR with the death toll highest in sub-Saharan Africa (Murray *et al.*, 2019). This data presents evidence for the dire need of therapeutics that are effective in slowing the development of AMR. Fortunately, antimicrobial peptides (AMPs) have emerged effective alternatives to antibiotics with increasing incentive for further development (Nguyen *et al.*, 2011). Numerous pathogens have contributed significantly to AMR especially in nosocomial settings. *Staphylococcus epidermidis* (*S. epidermidis*) is an example of a pathogen that spreads notoriously such settings and is thus the focus of this study.

The human skin microflora consists of numerous organisms that play a role in maintaining skin health. *S. epidermidis* is one of such that protects the host from bacterial invasion. Staphylococcus spp. are common commensal bacteria that colonise the human skin (Kloos, 1991). Staphylococci are Gram-positive, spore-forming, facultative anaerobic, and catalase positive organisms. Humans are first thought to encounter *S. epidermidis in utero* due to its presence in amniotic fluid. After birth, *S. epidermidis* colonises the skin and within a few days is a resident organism of the skin microbiota (Dominguez-Bello *et al.*, 2010).

S. epidermidis is an important commensal organism of the skin and mucosal membrane and aids in preventing infection from harmful microorganisms (Nguyen *et al.*, 2017). This organism secretes a number of factors that disrupts the attachment of invading pathogens. Despite the organism's beneficial role in skin health, *S. epidermidis* can also cause moderate to severe infection. These infections are common among immunocompromised individuals and are usually exacerbated by the formation of biofilms (Nguyen *et al.*, 2017). As a resident member of the skin microbiota, *S. epidermidis* easily evades host immune responses ensuring increased survival during infection (Otto, 2009). The treatment of infections caused by this organism is progressively worsened by resistance to numerous antibiotics allowing this pathogen to thrive in nosocomial settings (Fortuin-de Smidt *et al.*, 2015, Sabaté Brescó et al., 2017).

A study conducted by the Department of Biochemistry, Genetics, and Microbiology at the University of Pretoria identified a defensin isoform, OsDef2, present in the midgut of soft tick *Ornithodoros savignyi* (*O. savignyi*). OsDef2 was found to be active against Gram positive bacteria. *Owing to the high cost of OsDef2 synthesis, the C-terminus of the defensin was selected as a template for the shorter peptides and Os and Os-C was synthesised. Both analogues were bactericidal against Gram positive and Gram-negative bacteria causing acute cellular damage including the collapse of intracellular structures. Given the activity of these two peptides against other pathogens, this study sought to investigate the antibacterial activity and mode of action Os and Os-C against a clinically relevant strain of S. epidermidis.*

Methods and Materials

2.1 Bacterial strain

Polysaccharide intracellular adhesin-positive *S. epidermidis* (ATCC 35984) was used. Bacteria was grown aerobically in tryptic soy broth (TSB) at 37°C. Mid-logarithmic phase cells were obtained from overnight cultures diluted 100 times in TSB and proliferated until an OD_{600} of 0.327 was reached.

2.2 Preparation of synthetic peptides

The peptides Os and Os-C were synthesised using FlexiPeptide technology and were obtained from GenScript (New Jersey, USA). The purity and molecular mass of the peptides were determined by the manufacturer using reverse-phase high performance liquid chromatography and mass spectrometry, respectively. Melittin (Mel) (Sigma-aldrich, South Africa) was used as a positive control for membrane damage, identified in numerous studies. Lyophilised stocks of the peptide were dissolved in 300 µL of sterile deionised double distilled water. The peptides were then diluted, and their absorbance determined at 280 nm. Peptide concentration was determined using the following formula:

$$c = \frac{Mw \times\ df \times\ Abs}{n\,(\epsilon Tyr)\ +\ n\,(\epsilon Trp)}$$

Where c, is the concentration in mg/mL, MW is the molecular weight of each peptide, df is the dilution factor, and Abs is the absorbance at 280 nm. The extinction coefficients of tyrosine and tryptophan are 1200 and 5560 AU/mmol/mL, respectively (Lamichhane *et al.*, 2011).

2.3 Antibacterial Assays

The minimum inhibitory concentration (MIC) of Os and Os-C was determined using the method described by Nakajima *et al.*, (2003) and Prinsloo *et al.*, (2013) with some modification. *Staphylococcus epidermidis* was cultured overnight in TSB, diluted 100 times, and proliferated to an OD_{600} of 0.327. The cells were then centrifuged (5 000 × g for 10 minutes), washed twice with 10 mM sodium phosphate buffer (NaP) pH 6.6, and resuspended in 1% TSB. The washed culture was diluted to approximately 1×10^6 CFU/mL in 1% TSB. A volume of 90 µL of the cell suspension was treated with 10 µL of various peptide concentrations. The treated samples were incubated at 37°C in a shaking incubator for 6 hours and after incubation, 10 µL of 2.5 mM resazurin was added to each of the wells with further incubation in the dark for an hour. The fluorescence intensities were then measured using the SpectraMax Paradigm microplate reader (Molecular Devices, California, USA) at an excitation and emission wavelength of 535 nm and 590 nm respectively. The degree of inhibition was calculated thereafter.

The minimum bactericidal concentration (MBC) was determined by incubating *S. epidermidis* with three different concentrations of either peptide (10, 20, and 40 µM). An overnight culture was prepared, centrifuged, and washed as described in this section. The washed culture was diluted to approximately 1×10^6 CFU/mL in 1% TSB and treated with each peptide. The treated samples were incubated at 37°C in a shaking incubator for 6 hours. Following incubation, A volume of 100 µL of each sample was aspirated and plated directly onto tryptic soy agar (TSA) plates. Growth controls were prepared by diluting the untreated samples 500 times in 1% TSB. The agar plates were incubated at 37°C for 18 – 24 hours. The colonies formed on each plate were counted and the bactericidal activity of the samples was calculated using the following formula:

$$\%\ Killing\ =\ \left(1 - \frac{Observed\ no.\ of\ colonies\ in\ treated\ sample\ x\ df\ (growth\ control)}{Observed\ no.\ of\ colonies\ in\ untreated\ sample}\right) \times 100$$

The MBC was defined as the concentration at which 99.5% killing achieved.

2.4 Kinetics of Bactericidal Activity

A time-kill assay was performed using the method described by Boswell *et al.*, (1997) with slight modification. *Staphylococcus epidermidis* was prepared and diluted as described for the MBC determination. The cells were treated with each peptide at their respective MBCs. At specific time intervals (0, 60, 120, 180, 240, 300, and 360 min), 100 µL of the treated samples was plated directly onto TSA plates whereas the untreated samples (growth controls) were diluted 500 times in 1% TSB prior to transfer on TSA agar plates. The effective killing time of each peptide was defined as the time 99.5% killing was achieved.

2.5 Live/Dead Membrane Permeability Assay

Mid-logarithmic phase bacterial suspensions were diluted to a cell density of 1×10^8 CFU/mL in 1% TSB and treated with a concentration range of each peptide (melittin, Os, and Os-C) as described by the MIC determination method in 2.3. Inhibition, however, was assessed for 2 hours to avoid cell death due to nutrient depletion. Following the determination of the inhibitory activity of each peptide at a cell density of 1×10^8 CFU/mL, sub-inhibitory concentrations that caused 30% inhibition of *S. epidermidis* growth were used for the mode of action experiments.

To quantify membrane permeabilisation, the Live/Dead assay was performed according to the manufacturer's instructions using the L7007 LIVE/DEAD® BacLight Bacterial viability kit (ThermoFisher, Johannesburg, South Africa) with slight modification. Mid-logarithmic phase bacterial suspensions were diluted to a cell density of 1 x 10^8 CFU/mL in 1% TSB and treated with 0.4 µM melittin, 7 µM Os, or 20 µM Os-C for 2 hours at 37°C. A 2X staining solution of the Live/Dead dye was then prepared in 2 mL of double distilled and deionised water. A volume of 100 µL of the stain was then added to all the wells and further incubated in the dark at room temperature for 15 minutes. The fluorescence intensities were then measured at an excitation and emission wavelength of 485 nm and 530 nm (green fluorescence) and an excitation and emission wavelength of 485 nm and 630 nm respectively (red fluorescence). The ratio was computed as follows:

$$\frac{Live}{Dead}Ratio = \frac{Green\ Fluoresence}{Red\ Fluoresence}$$

2.6 Membrane Depolarisation Assay

Membrane depolarisation was assessed using the method described by Zoric *et al* (2015). Mid-logarithmic phase bacterial suspensions were diluted to a cell density of 1 × 10^8 CFU/mL in 1% TSB and treated with 0.4 µM melittin, 7.0 µM Os, or 20 µM Os-C for 2 hours at 37°C. The samples were subsequently incubated with 100 µL of 20 µg/mL (final concentration) of $DiBAC_4(3)$ for 1 hour at 37°C with continuous shaking at 160 rpm. $DiBAC_4(3)$ stimulated the attachment of cells to the 96-well plate. Dead/unattached cells were removed by performing 2 separate washes using 100 µL of ice-cold phosphate-buffered saline (PBS) pH 7.4. The fluorescence was then measured at an excitation and emission wavelength of 490 nm and 516 nm, respectively.

2.7 Scanning Electron Microscopy

The sample preparation methods described by Taute (2017) were adapted for this study. *S. epidermidis* cultures were prepared and the mid-logarithmic phase culture was diluted to a cell density of 1x10^8 CFU/mL in 1% TSB. The cells were then treated with a final concentration of 0.4 µM melittin, 7 µM Os, and 20 µM Os-C. The samples were treated with the peptides for 2 hours at 37°C with constant shaking at 160 rpm. After treatment, a volume of 100 µL of the samples were transferred to the poly-L-lysine coated coverslips and were allowed to adhere for 1 hour. The samples mounted on to the coverslips were then rinsed twice with 0.075 M phosphate buffer, pH 7.4 for 10 minutes to remove unbound cells. The cells were immediately fixed in a 2.5% glutaraldehyde and 2.5% formaldehyde solution in 0.075 M phosphate buffer, pH 7.4 for 1 hour. Following chemical fixation, the samples were rinsed three times in 0.075 M phosphate buffer, pH 7.4 for 10 minutes. A 1% osmium tetroxide solution was used as a secondary chemical fixative and was therefore added to the samples for 30 minutes. The samples were rinsed three times in 0.075 M phosphate buffer, pH 7.4 for 10 minutes. The samples were then serially dehydrated in 30%, 50%, 70%, 90%, and three changes of 100% ethanol for 15 minutes. The dehydrated samples were then dried in hexamethyldisilane (HMDS), mounted with carbon tape onto aluminium stubs, carbon coated and viewed with an Ultra plus field emission gun (FEG) SEM (Zeiss, Oberkochen, Germany).

2.8 Transmission Electron Microscopy

The samples were processed for viewing using the method described by Bozzola (2014) with slight modification. *S. epidermidis* cells in the exponential phase were adjusted to a cell density of 1x10^8 CFU/mL. A volume of 900 µL of the cells were subsequently treated with 100 µL of 7 µM Os, 20 µM Os-C, and 0.4 µM

melittin for 2 hours. The cells were then centrifuged with an equal volume warm fixative, 4% formaldehyde and 2.5% glutaraldehyde at 5000 × g. The cells were then fixed with a 4% formaldehyde/ 2.5% glutaraldehyde solution in 0.075 M phosphate buffer, pH 7.4 for 4 hours. The cells were then rinsed three times in the same buffer for 15 minutes. Thereafter, the cell suspensions were fixed in a 1% osmium tetroxide solution overnight and then rinsed again in 0.075 M phosphate buffer, pH 7.4 as described after primary fixation.

An agarose solution was prepared by dissolving 0.4 g of agarose powder (Sigma-Aldrich, Johannesburg) in 10 mL of pre-heated double distilled deionised water. The liquid agarose suspension was then cooled to a temperature of 45°C and the cells were suspended in the solution and placed in ice for 15 minutes to promote quicker solidification. The solidified samples were then cut into 1- 2 mm cubes and were rinsed several times in 0.075 M phosphate buffer, pH 7.4. The cubes were then serially dehydrated in 30%, 50%, 70%, 90%, and three changes of 100% ethanol for 15 minutes. The cells were infiltrated with 50% Embed 812 Resin (SPI supplies, Pennsylvania, USA) for 2 hours followed by 100% resin overnight. The resin was then replaced and polymerised into moulds for 72 hours at 60°C. Ultrathin 100 nm sections were made with the Lecia Ultramicrotome (Lecia Microsystems GmbH, Wetzlar, Germany) using a 45° diamond knife (Diatome, Pennsylvania, USA). The sections were picked up on copper grids and contrasted with 4% aqueous uranyl acetate and Reynold's lead citrate solution. The copper grids were rinsed in water and the sections were viewed on the JEM-2100F TEM (JEOL, Tokyo, Japan).

Results

3.1 Antibacterial Activity

The antibacterial activity of Os and Os-C was assessed in 1% TSB. Both peptides were active against *S. epidermidis*. The MIC of Os was 10 ± 0.00 μM and for Os-C was 3.43 ± 0.71 μM while both peptides were bactericidal at 10 μM (Figure 1 A,B). The effective killing time was defined as the point where 99.5% killing was observed and this was seen after 3 hours following treatment to either Os or Os-C.

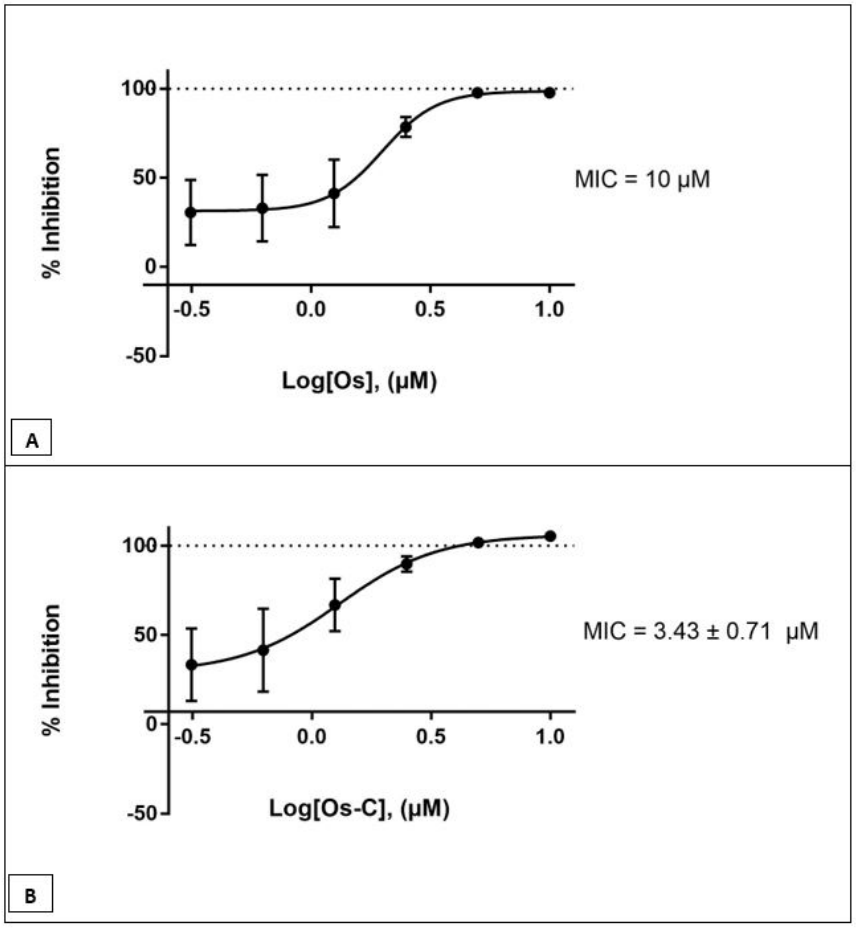

Figure 1: The inhibitory activity of A)Os and B)Os-C against *S. epidermidis* in 1% TSB. Mid-logarithmic phase *S. epidermidis* cells were exposed to two-fold dilutions of either Os or Os-C for 6 hours. Viability was measured using 2.5 mM resazurin. Error bars indicate the Standard Error of the Mean (SEM) of three independent experiments performed in triplicate.

The antibacterial activity of both peptides against *S. epidermidis* is summarised in Table 1.

Peptide	MIC (μM)	MBC (μM)	Killing Time (hrs)
Os	10.0	10.0	3
Os-C	3.23	10.0	3

Table 1: A summary of the antibacterial activity of both peptides against *Staphylococcus epidermidis*

3.2 Membrane Permeability and Depolarisation

The bacterial cell membrane remains one of the most targeted cell components for AMPs. To effectively conduct the mode of action studies, the cell density was augmented to facilitate sufficient uptake of the fluorescent dyes. Prior to analysis using the different fluorescent probes the inhibitory activity of melittin (peptide control), Os, and Os-C was assessed at 1×10^8 CFU/mL. Sub-inhibitory concentrations of each peptide that caused 30% inhibition in growth were chosen for the subsequent experiments. Melittin caused 30% inhibition at 0.4 μM whereas Os and Os-C achieved the same at 7 μM and 20 μM, respectively (Figure 2).

The Live/Dead assay was used to measure membrane permeability indicated by the Live/Dead ratio produced following treatment with either peptide. A ratio equal to 3 was seen with the untreated cells, which according to the kit protocol was indicative of a sample where 100% of the cell population was viable and thus presented with intact membranes. The Live/Dead ratio produced by melittin, and Os was 1.35 and 0.93, respectively and was therefore significantly different when compared to the untreated control (Figure 3A). Os-C, however produced a ratio that was not significantly different from the untreated control. This revealed that Os, like melittin, when compared to Os-C caused membrane permeabilisation whereas Os-C had a different mode of action.

The ability of melittin, Os, and Os-C to induce a change in membrane potential was also investigated using a fluorescent membrane potential sensitive dye, $DiBAC_4(3)$. Analysis into the polarity of the membrane revealed that there was no significant difference in the fluorescence intensity between melittin and the untreated sample. Os and Os-C, however, displayed a significant increase in fluorescence when compared to the untreated control suggesting that both peptides caused membrane depolarisation (Figure 3B). While both peptides appeared to cause membrane depolarisation, Os-C produced a fluorescence signal that was almost twice that produced by Os.

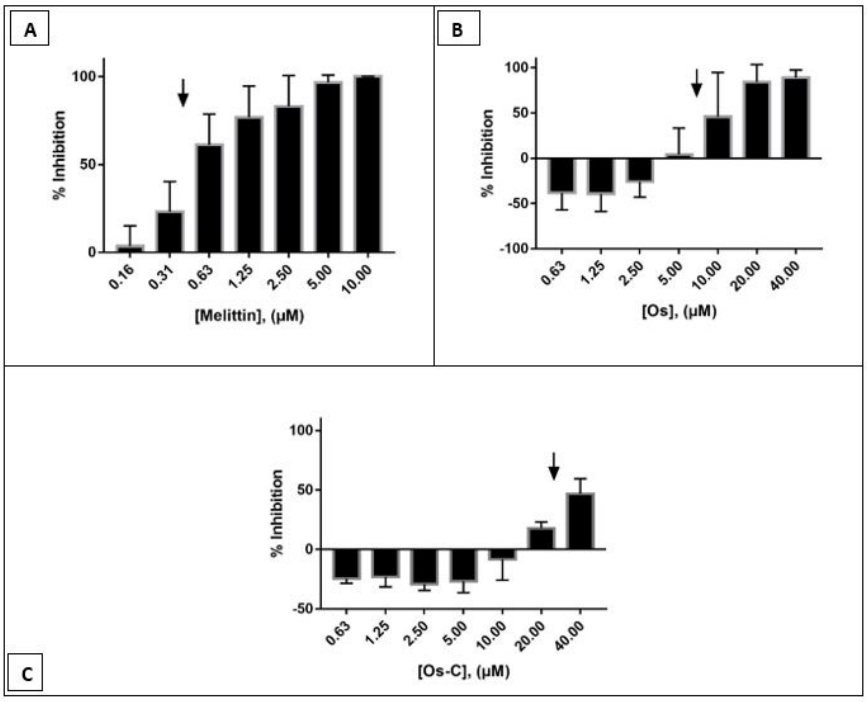

Figure 2: The inhibitory activity of A) Mel, B) Os, and C) Os-C at a cell density of 1 x 10^8 CFU/mL. The modified microbroth dilution was performed to analyse a change in the activity of the peptides following the subsequent increase in the density of *S. epidermidis*. Arrows indicate the concentrations of the peptides where 30% inhibition of growth was achieved after 2 hours. Error bars indicate the SEM of two independent experiments performed in triplicate.

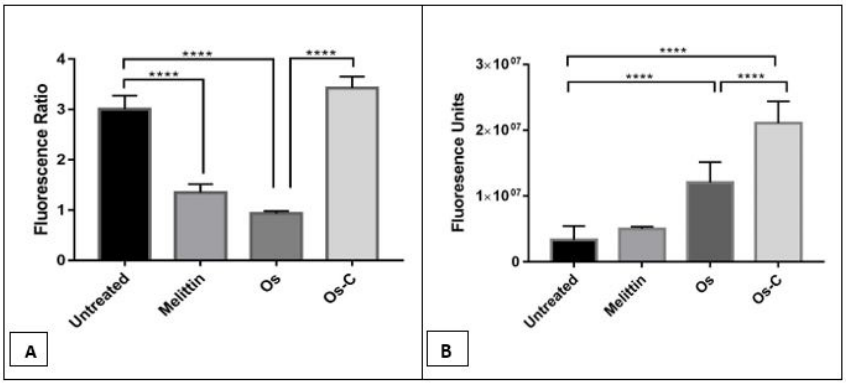

Figure 3: The Analysis of the degree of *Staphylococcus epidermidis* membrane permeabilisation and depolarisation. Mid-logarithmic phase *S. epidermidis* cells (1×10^8) were exposed to sub-inhibitory concentrations of Mel (0.4 µM), Os (7 µM), or Os-C (20 µM) for 2 hours. A) Membrane permeabilisation was analysed using a SYTO 9/PI staining solution. B) Depolarisation was investigated using the slow-response potential-sensitive dye $DiBAC_4(3)$. Error bars indicate the SEM with significant differences indicated by *, **, ***, and **** representing $p < 0.05$, $p < 0.01$, $p < 0.001$, and $p < 0.0001$ respectively. Results are of three independent experiments performed in triplicate.

3.3 Scanning Electron Microscopy

The effects of melittin, Os, and Os-C on *S. epidermidis* cells was evaluated using scanning electron microscopy. The untreated bacterial cells displayed a typical round morphology with relatively smooth membrane surfaces. The cells were further characterised by well-defined division septa (Figure 4A, B) and the formation of a tetrad (Figure 4B) which are noted as definitive hallmarks of cell proliferation. Treatment with 0.4 µM melittin revealed altered cell morphologies with some colonies appearing irregular in shape laden with membrane indents (Figure 4C). Melittin was also shown to stimulate biofilm formation visible through the formation of multilayer cell agglomerates adjoined by tight contact cell-cell junctions in addition to membrane blebs and bacterial ghosts (Figure 4C, D).

Bacterial cells treated with Os displayed rougher membrane surfaces with progressively larger membrane blebs (Figure 4E). Exposure to the peptide also caused the deposition of amorphous material appearing as extracellular vesicles. Like melittin, Os also induced the formation of ghost cells in addition to membrane indents (Figure 4E, F). In contrast to Os, Os-C had relatively smoother membrane surfaces. Os-C, however, also formed membrane blebs in addition to the deposition of debris that appear smaller than those deposited by Os (Figure 4G, H). Treatment with Os-C also stimulated the formation of extended structures protruding from the *S. epidermidis* cell membrane (Figure 4G).

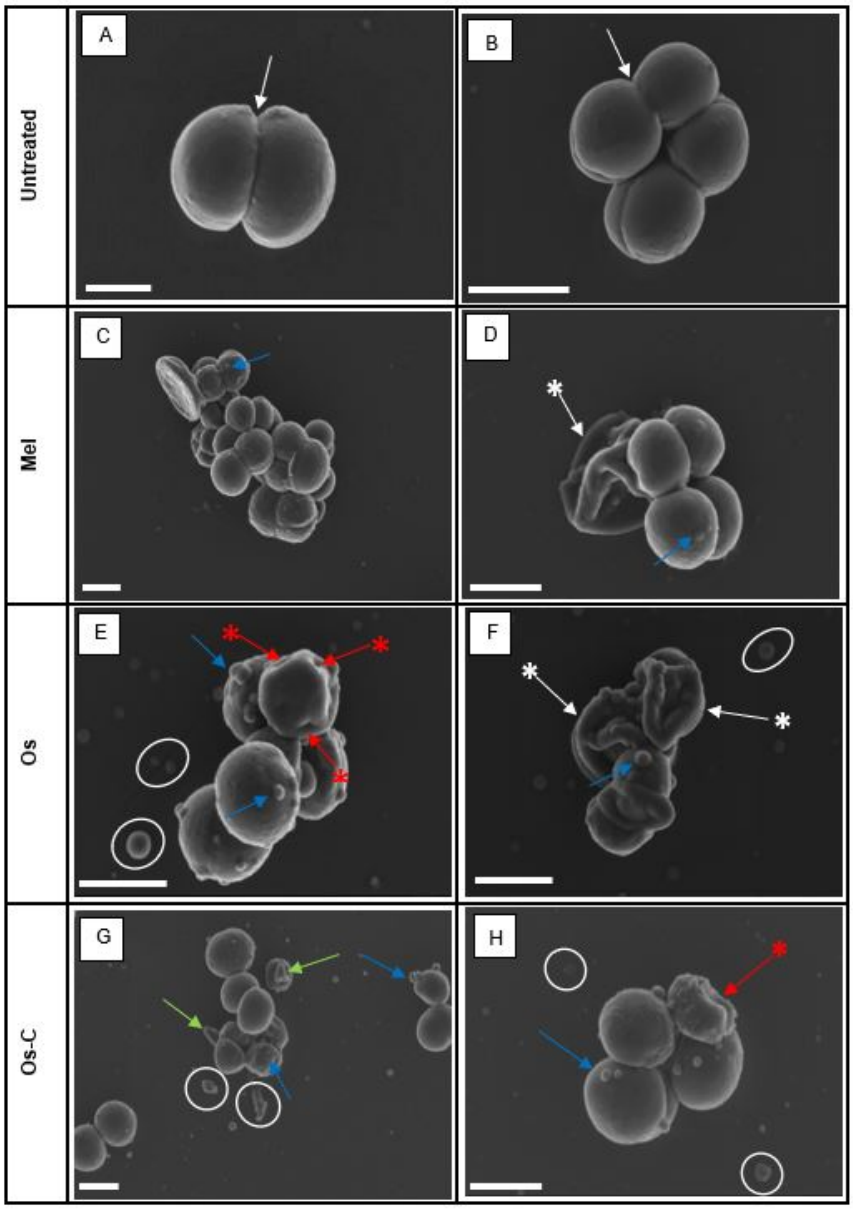

Figure 4: The morph ological effects of Mel, Os, and Os-C on *S. epidermidis.* Mid-logarithmic phase cells were exposed to sub-inhibitory concentrations of the three peptides for 2 hours and analysed using scanning electron microscopy. White arrows indicate division septa, blue arrows indicate membrane blebs, green arrows indicate membrane protrusions, white asterisks with adjacent arrows indicate bacterial ghosts, red asterisks with adjacent arrows indicate membrane indents, and white ovals cellular debris or amorphous material. Scale bars = 1 μm.

3.4 Transmission Electron microscopy

S. epidermidis cells treated with melittin, Os, or Os-C were also evaluated using transmission electron microscopy. Untreated cells displayed intact and well-defined cell walls and membrane. The cells also displayed characteristic division septa including intracellular homogeneity (Figure 5A, B). Cells treated with melittin displayed irregular septa in addition to surface indents (Figure 5C). The peptide also had an effect on the bacterial cell wall causing the fragmentation of cell wall components and cytoplasmic retraction (Figure 5D).

Cells treated with Os also produced irregular septa also bearing an effect on the cell wall components. Os was further shown to cause cell lysis, intracellular coagulation, and the extrusion of intracellular material (Figure 5E, F). In contrast, Os-C caused intracellular invagination, thicker irregular septa, and mesosome formation (Figure 5G, H).

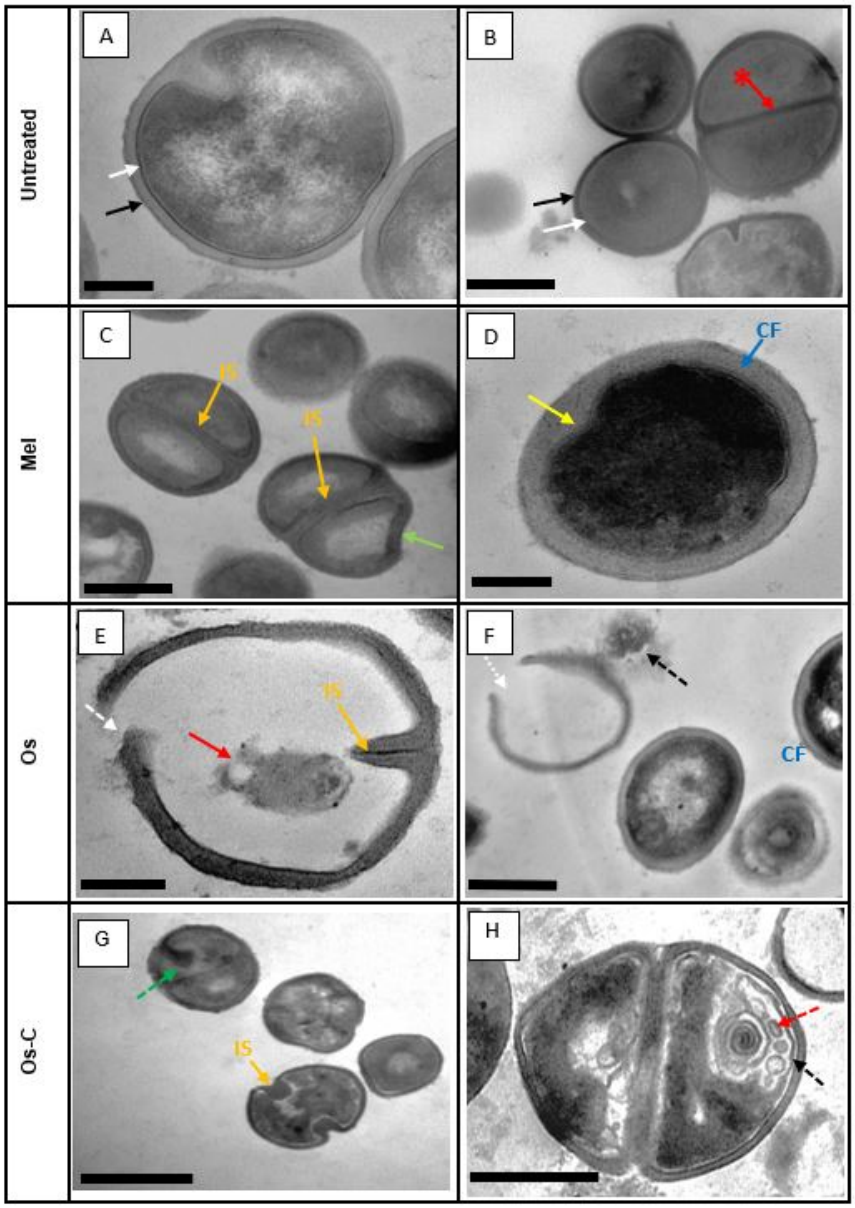

Figure 5: The effects of Mel, Os, and Os-C on *S. epidermis* ultrastructure. Mid-logarithmic phase cells were exposed to sub-inhibitory concentrations of the three peptides for 2 hours and analysed using scanning electron microscopy. Black arrows indicate the bacterial cell wall, white arrows indicate the cell membrane, division septa are indicated by red asterisks with adjacent arrows, irregular septation (IS) is indicated by orange arrows, light green arrows indicate membrane indentation, yellow arrows indicate cytoplasmic retraction, blue arrows indicate cell wall fragmentation (CF), solid red lines indicate coagulated material, broken white lines indicate cell lysis, broken black lines indicate mesosomes, and broken red lines indicate mesosome tubules. Scale bars A, D, and E = 200 nm. B, C, F, and H = 500 nm. G = 1000 nm.

Discussion

Antimicrobial peptides remain promising alternatives to conventional antibiotics. Their broad spectrum of activity in addition to their varied modes of action make it less probable that pathogens develop resistance against these novel compounds. Overtime, this will ease the burden on health systems fueled by the unprecedented increase in AMR cases globally. This study evaluated the antibacterial activity and mode of action of defensin-derived AMPs Os and Os-C against *S. epidermidis*. The antibacterial activity of these two peptides was determined in low nutrient media due to their sensitivity to high salt and protein concentrations. More specifically, Prinsloo *et al.*, (2013) showed that Os and Os-C were inactive against *E. coli* and *B. subtilis* in Mueller Hinton Broth and Luria-Bertani Broth. Similarly, Mbuayama (2016) reveled that the antifungal activity of both peptides was lost in high salt concentrations. Several studies have attributed this to the net charge of AMPs at pH 7. Shafee *et al.*, (2017) and Kerenga *et al.,* (2019) showed that AMPs with a high net charge at pH 7 were stable in media laden with a high concentration of salts and proteins. For this purpose, minimal nutrient media was used to avoid further modification of the peptides used in this study.

Both Os and Os-C were active against *S. epidermidis* in 1% TSB. The MIC of Os and Os-C was equal to 3.43 ± 0.71 μM almost three times higher than Os (10.00 μM). The MBC and effective killing time of both peptides was subsequently determined. It was shown that both peptides had an MBC equal to 10 μM and an effective killing time of three hours. The equal MIC and MBC values displayed by Os indicated that the peptide possibly needed to reach a threshold concentration before exerting potent activity. Os-C, however, was able to inhibit bacterial growth at lower concentrations perhaps through a different mode action and at its MBC (10 μM) caused killing within a three-hour period. Prinsloo *et al.*, (2013) showed that the MBC of Os and Os-C against *S. aureus* was 6.10 μM and 6.98 μM respectively. *S. aureus* and *S. epidermidis* are closely related organisms that potentially share the same virulence factors necessary to cause infection (Jiménez *et al.,* 2011). The MBC values obtained for *S. aureus* are thus comparable to those obtained in this study using *S. epidermidis*.

The mode of action of both peptides was also investigated. Numerous AMPs have been shown to function by direct means and therefore act directly on bacterial cell membranes (Nguyen *et al.,* 2011, Kumar *et al.,* 2018). This study therefore evaluated whether Os and Os-C were membrane acting. To achieve this, the Live/Dead membrane permeability kit and membrane potential sensitive dye $DiBAC_4(3)$ was used. The Live/Dead membrane permeability kit incorporates the use of a nucleic acid stain and therefore requires a higher cell density. The cell density was thus increased and maintained throughout the study. Due to the inoculum effect (Brook, 1989), a principle that describes the decrease in activity of an antimicrobial agent following an increase in cell density, the antibacterial activity of both peptides including melittin, the peptide control, had to be determined. Furthermore, sub-inhibitory concentrations of each peptide that caused 30% inhibition in bacterial growth was used. The rationale for this decision is presented by numerous studies reporting improved characterisation of peptide action at lower concentrations where killing is sequential and not too rapid as compared to the MIC_{50} of a peptide or a higher concentration (Patrzykat *et al.*, 2002, Aisenbery *et al.,* 2019, Yin *et al.*, 2019).

Melittin caused 30% inhibition in *S. epidermidis* growth at 0.4 μM whereas Os and Os-C achieved that at 7 μM and 20 μM respectively. These concentrations were subsequently used to analyse whether the two peptides (Os and Os-C) caused membrane permeabilisation with melittin, a known lytic peptide (Nam *et al.*, 2018) used as a positive control. The Live/Dead assay revealed that only melittin and Os caused membrane permeabilisation. Boix-Lemonche *et al.*, (2020) showed that melittin caused permeabilisation of the same strain of *S. epidermidis* used in this study at concentrations as low as 0.125 μM. Os-C, however, did not cause membrane permeabilisation at the concentration used (20 μM). This finding may be attributed to the structure and physicochemical properties of Os-C that largely influences the interaction with the organism. Melittin has been classified as an α-helical peptide (Vogel & Jähnig, 1986, Nguyen *et al.*, 2011, Prinsloo, 2013) and has been shown to interact with microbial membranes through the formation of toroidal pores (Brogden, 2005). Structural characterisation of Os and Os-C revealed that Os adopted a partial α-helical structure with extended coils and the latter a partial β-sheet with extended coils (Prinsloo *et al.*,

2013). The difference in structure, therefore, presents the possibility of a different mode of action.

The effects of both peptides on membrane potential were also investigated. Melittin was shown to have no effect on membrane potential whereas Os and Os-C caused membrane depolarisation, a positive shift in membrane potential, at the concentrations used. Although melittin caused membrane permeabilisation, its inability to cause membrane depolarisation was also observed by Boix-Lemonche *et al.*, (2020) at concentrations as low as 0.125 μM. This was attributed to reversible membrane damage caused by the otherwise potent peptide at low concentrations. Analogously, Os caused membrane depolarisation which was a consequence of irreversible membrane damage seen after visualising cells using transmission electron microscopy (Figure 5 E,F). Membrane permeabilisation was therefore identified as a key even in the mode of action of Os.

Further visualisation of the cells using scanning and transmission electron microscopy revealed that all the three peptides had adverse effects on the membrane of *S. epidermidis*. More specifically, melittin caused membrane indentation, blebbing, and ghost cell formation in addition to irregular septation. Os and Os-C similarly caused membrane blebbing with Os also inducing the formation of bacterial ghosts. Os was further shown to be lytic causing intracellular coagulation and due to membrane lysis, the extrusion of such intracellular material. This confirms the initial observations into the membrane targeting ability of Os. Os-C, however, was shown to induce mesosome formation. Grigor'eva *et al.*, (2020) suggested that mesosome formation was an event stimulated by membrane damage due to reactive oxygen species (ROS) production. Grigor'eva *et al.*, (2020) further revealed that prolonged exposure of *S. aureus* to R9F2, a synthetic AMP, caused osmiophilia (high affinity for osmium tetroxide staining) in mesomes which was cited to be a hallmark of acute cellular damage linked to ROS production. Previously, Mbuayama (2016) showed that Os-C induced endogenous ROS production in *C. albicans*. Os-C, therefore, could be causing membrane damage via indirect means, possibly through the generation of ROS. This can be evaluated in a future study using the method described by Lupetti *et al.*, (2002) to monitor endogenous ROS production.

In conclusion, Os and Os-C are active against *S. epidermidis* causing cell death through different mechanisms. The bacterial membrane remains an essential target for these two peptides enabling them to further interact with their downstream targets. While Os directly targets the *S. epidermidis* membrane, Os-C possibly targets the membrane in addition to intracellular structures indirectly possibly through ROS formation. The susceptibility of these peptides to high salt concentrations can be overcome by several modifications for systemic use in otherwise severe cases of infection. The nature of most of the infections caused by *S. epidermidis*, however, are either superficial or on surgical site wounds. This study therefore proposes the use of these peptides (with greater focus on Os) for topical application to treat superficial infections caused by the organism or as an AMP to facilitate wound healing and repair. In both scenarios, this peptide could effectively prevent serious infection and reduce the spread of *S. epidermidis* in clinical settings.

Acknowledgments

We acknowledge the Department of Biochemistry Genetics and Microbiology in addition to the Section of Cell Biology and Histology under the Department of Anatomy at the University of Pretoria for funding and enabling the study.

References

Aisenbrey, C., Marquette, A. and Bechinger, B., 2019. The mechanisms of action of cationic antimicrobial peptides refined by novel concepts from biophysical investigations. Antimicrobial Peptides. 1:33-64.

Boix-Lemonche, G., Lekka, M. and Skerlavaj, B., 2020. A rapid fluorescence-based microplate assay to investigate the interaction of membrane active antimicrobial peptides with whole Gram-positive bacteria. Antibiotics. 9(2):1-16.

Boswell, F.J., Sunderland, J., Andrews, J.M. and Wise, R., 1997. Time-kill kinetics of quinupristin/dalfopristin on *Staphylococcus aureus* with and without a raised MBC evaluated by two methods. The Journal of Antimicrobial Chemotherapy. 39(1):29-32.

Bozzola, J. J. (2014). Conventional specimen preparation techniques for transmission electron microscopy of cultured cells. In Electron Microscopy. Humana Press, Totowa, NJ.

Brogden, K.A. 2005. Antimicrobial peptides: pore formers or metabolic inhibitors in bacteria? Nature Reviews Microbiology. 3(3):238-250.

Brook, I., 1989. Inoculum effect. Reviews of Infectious Diseases. 11(3):361-368.

Dominguez-Bello, M.G., Costello, E.K., Contreras, M., Magris, M., Hidalgo, G., Fierer, N. and Knight, R., 2010. Delivery mode shapes the acquisition and structure of the initial microbiota across multiple body habitats in newborns. Proceedings of the National Academy of Sciences. 107(26):11971-11975.

Grigor'eva, A., Bardasheva, A., Tupitsyna, A., Amirkhanov, N., Tikunova, N., Pyshnyi, D. and Ryabchikova, E., 2020. Changes in the ultrastructure of *Staphylococcus aureus* treated with cationic peptides and chlorhexidine. Microorganisms 8(12):1-19.

Jiménez, J.N., Ocampo, A.M., Vanegas, J.M., Rodríguez, E.A., Garcés, C.G., Patiño, L.A., Ospina, S. and Correa, M.M., 2011. Characterisation of virulence genes in methicillin susceptible and resistant Staphylococcus aureus isolates from a paediatric population in a university hospital of Medellin, Colombia. Memórias do Instituto Oswaldo Cruz. 106(1):980-985.

Kerenga, B.K., McKenna, J.A., Harvey, P.J., Quimbar, P., Garcia-Ceron, D., Lay, F.T., Phan, T.K., Veneer, P.K., Vasa, S., Parisi, K. and Shafee, T., 2019. Salt-tolerant antifungal and antibacterial activities of the corn defensin ZmD32. Frontiers in Microbiology.10(1):1-35.

Kloos, W. 1991. The genus staphylococcus. The Prokaryotes. A Handbook on the Biology of Bacteria: Ecophysics, Isolation, Identification, Application. Athens, GA, Springer Science & Business Media. p. 1369-1420.

Kumar, P., Kizhakkedathu, J.N. and Straus, S.K., 2018. Antimicrobial peptides: diversity, mechanism of action and strategies to improve the activity and biocompatibility in vivo. Biomolecules. 8(4):1-24.

Lamichhane, T.N., Abeydeera, N.D., Duc, A.C.E., Cunningham, P.R. and Chow, C.S., 2011. Selection of peptides targeting helix 31 of bacterial 16S ribosomal RNA by screening M13 phage-display libraries. Molecules. 16(2):1211-1239.

Lupetti, A., Paulusma-Annema, A., Senesi, S., Campa, M., Van Dissel, J.T. and Nibbering, P.H., 2002. Internal thiols and reactive oxygen species in candidacidal activity exerted by an N-terminal peptide of human lactoferrin. Antimicrobial Agents and Chemotherapy. 46(6):1634-1639.

Mbuayama, K. R. 2016. Antifungal properties of peptides derived from a defensin from the tick *Ornithodoros savignyi*. MSc Dissertation. University of Pretoria.

Murray, C.J., Ikuta, K.S., Sharara, F., Swetschinski, L., Aguilar, G.R., Gray, A., Han, C., Bisignano, C., Rao, P., Wool, E. and Johnson, S.C., 2022. Global burden of bacterial antimicrobial resistance in 2019: a systematic analysis. The Lancet. 399:629-655

Nam, J., Yun, H., Rajasekaran, G., Kumar, S.D., Kim, J.I., Min, H.J., Shin, S.Y. and Lee, C.W., 2018. Structural and functional assessment of mBjAMP1, an antimicrobial peptide from *Branchiostoma japonicum*, revealed a novel α-hairpinin-like scaffold with membrane permeable and DNA binding activity. Journal of Medicinal Chemistry. 61(24):11101-11113.

Nguyen, L.T., Haney, E.F. and Vogel, H.J. 2011. The expanding scope of antimicrobial peptide structures and their modes of action. Trends in Biotechnology. 29(9):464-472.

Nguyen, T.H., Park, M.D. and Otto, M. 2017. Host response to *Staphylococcus epidermidis* colonization and infections. Frontiers in Cellular and Infection Microbiology. 7(1):1-7.

Nakajima, Y., Ishibashi, J., Yukuhiro, F., Asaoka, A., Taylor, D. and Yamakawa, M. 2003. Antibacterial activity and mechanism of action of tick defensin against Gram-positive bacteria. Biochimica et Biophysica Acta (BBA)-General Subjects. 1624(1-3):125-130.

Patrzykat, A., Friedrich, C.L., Zhang, L., Mendoza, V. and Hancock, R.E., 2002. Sublethal concentrations of pleurocidin-derived antimicrobial peptides inhibit macromolecular synthesis in *Escherichia coli*. Antimicrobial Agents and Chemotherapy. 46(3):605-614.

Prinsloo, L., Naidoo, A., Serem, J., Taute, H., Sayed, Y., Bester, M., Neitz, A., Gaspar, A. 2013. Structural and functional characterization of peptides derived from the carboxy-terminal region of a defensin from the tick *Ornithodoros savignyi*. Journal of Peptide Science. 19(5):325-332.

Taute, H. 2017. The mode of action of the synthetic peptides Os and Os-C derived from the soft tick *Ornithodoris Savignyi*. Doctoral thesis. University of Pretoria.

Shafee, T., Lay, F.T., Phan, T.K., Anderson, M.A. and Hulett, M.D., 2017. Convergent evolution of defensin sequence, structure and function. Cellular and Molecular Life Sciences. 74(4):663-682.

Vogel, H. and Jähnig, F., 1986. The structure of melittin in membranes. Biophysical Journal. 50(4):573-582.

Yin, D., Wu, S., Yang, Y., Shi, Q., Dong, D., Zhu, D. and Hu, F., 2019. Results from the China Antimicrobial Surveillance Network (CHINET) in 2017 of the in vitro activities of ceftazidime-avibactam and ceftolozane-tazobactam against clinical isolates of Enterobacteriaceae and Pseudomonas aeruginosa. Antimicrobial Agents and Chemotherapy. 63(4):2431-2449.

Zorić, N., Kosalec, I., Tomić, S., Bobnjarić, I., Jug, M., Vlainić, T. and Vlainić, J. 2017. Membrane of *Candida* albi*cans* as a target of berberine. BMC Complementary and Alternative Medicine. 17(1)**:**1-10